Statistical Analysis and Predictability of Large Scale Travelling Ionospheric Disturbances

C. Borries[1], A.A. Ferreira[1], R.A. Borges[2]

1) German Aerospace Center (DLR), Neustrelitz, Germany
2) University of Brasilia, Brasilia, Brasil

State of the Art

Can we predict the occurrence and amplitude of LSTIDs?

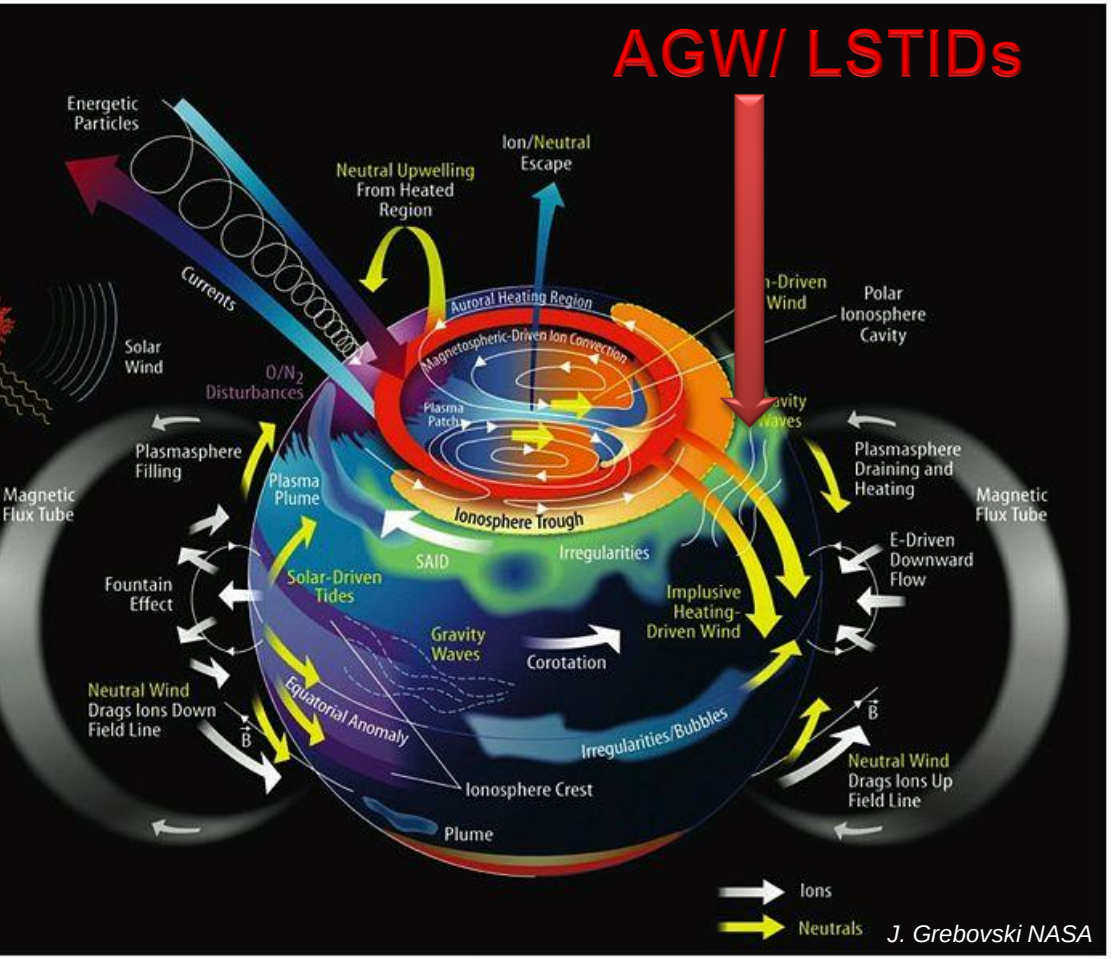

Tsugawa+(2004)

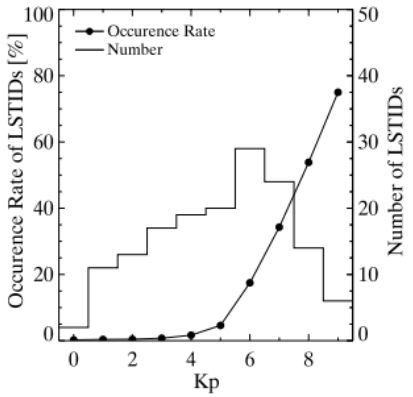

Figure 2. The occurrence rate ξ (%/3 hours) (solid circles) and the number N_A of the LSTIDs (histogram) against *Kp* index. Here ξ for the *Kp* value was defined as the probability that one LSTID appears over Japan during a 3-hour period with the *Kp* value. The occurrence rate increased as the *Kp* value increased, that is, 1% at $Kp = 4$ and 75% at $Kp = 9$. The number of the LSTIDs under geomagnetically quiet conditions, $Kp \leq 3$, was 43, that is, 28% of all the LSTIDs.

Czerniak & Zakharenkova (2018)

We found that an equatorward expansion of the strong ionospheric irregularities zone and an increase of the FACs magnitude led to a simultaneous intensification of the LSTIDs occurrence at high latitudes.

Borries+(2009)

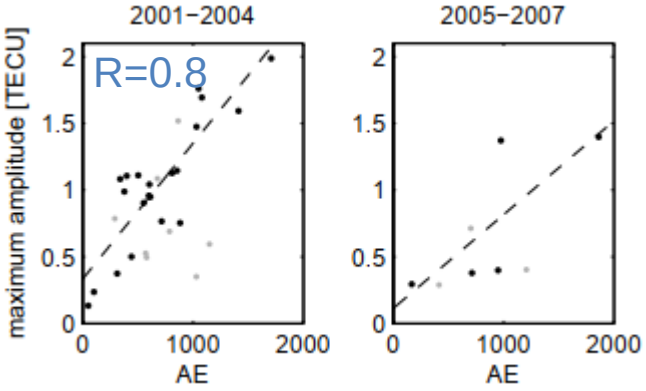

Afraimovich+(2001)

3. It was found that an increase in the level of geomagnetic activity is accompanied by an increase in the total intensity of TEC; however, it does not correlate with the absolute level of *Dst*, but rather with the value of the time derivative of *Dst* (a maximum correlation coefficient reaches −0.94).

Ding+(2008)

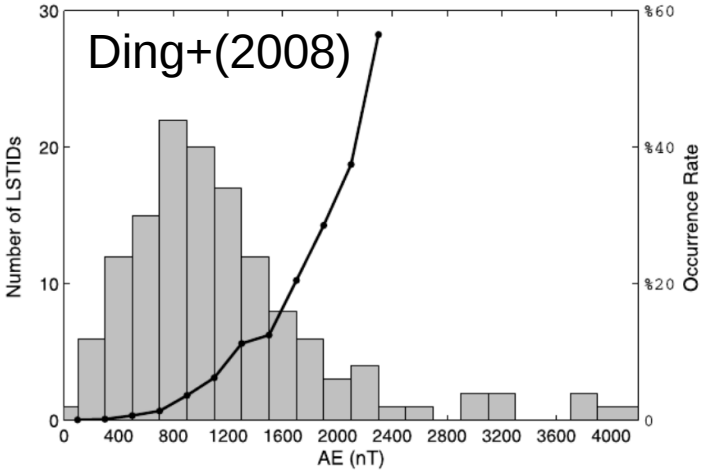

Figure 4. The histogram of the number of LSTID events against AE index (gray bars), and the change of occurrence rate with AE index (black curve).

TID Activity Index

- Step 1: common TID derivation from ground based Total Electron Content (TEC) measurements

$$TECp(t) = TECv(t) - \frac{1}{T}\sum_{n=t-0.5T}^{t+0.5T} TECv(n)$$

- Step 2: TID activity index

$$A_{TID}(t) = 0.5(\max_x(TECp(x) * F(x-t)) - \min_x(TECp(x) * F(x-t)))$$

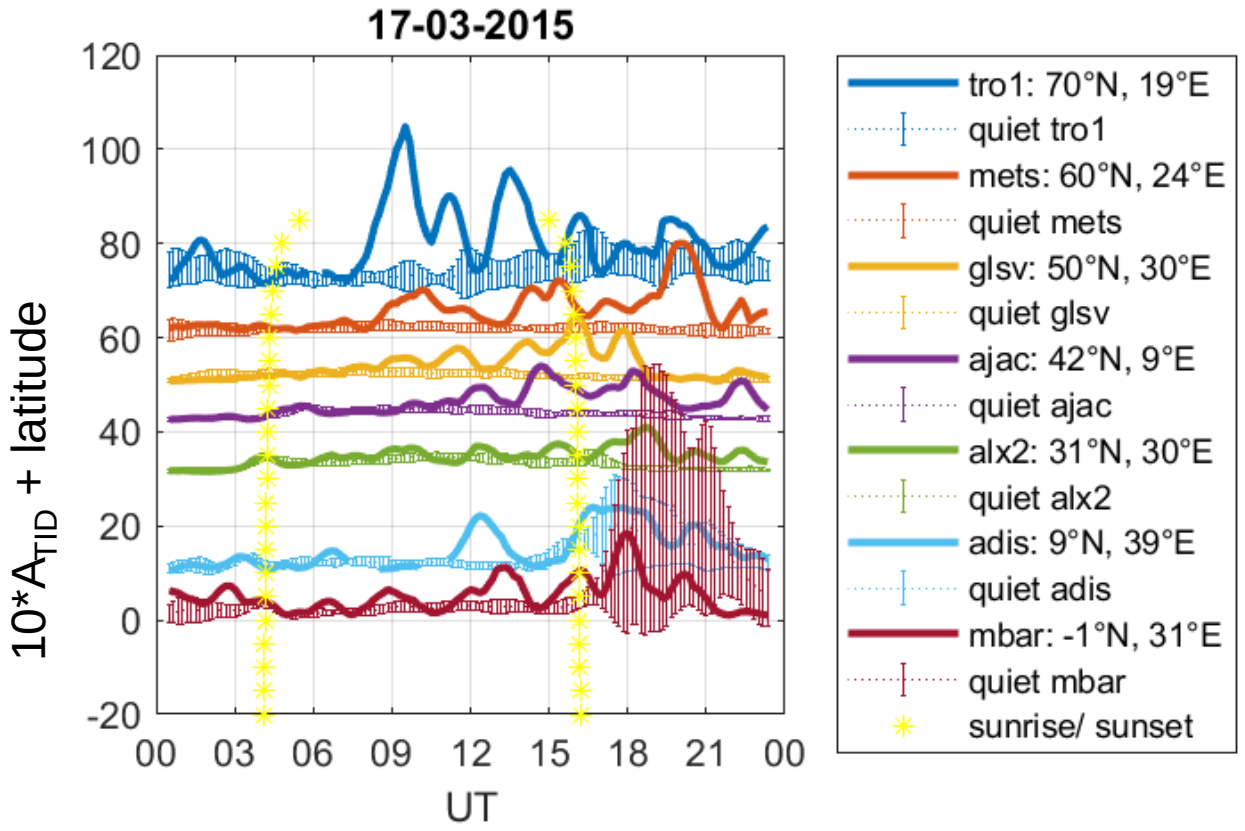

Parameter selection

Newell+(2007, doi: 10.1029/2006ja012015)

Table 1. Twenty Candidate Solar Wind-Magnetosphere Coupling Functions and Their Origins in Roughly Historical Order

Name	Functional Form	Reference
B_z	B_z	*Dungey* [1961]
Velocity	v	*Crooker et al.* [1977]
Density	n	
p	$nv^2/2$	*Chapman and Ferraro* [1931]
Bs	B_z ($B_z < 0$); 0 ($B_z > 0$)	
Half-wave rectifier	vBs	*Burton et al.* [1975]
ε	$vB^2\sin^4(\theta_c/2)$	*Perrault and Akasofu* [1978]
ε_2	$vB_T^2\sin^4(\theta_c/2)$	Variant on ε
ε_3	$vB\sin^4(\theta_c/2)$	Variant on ε
Solar wind E-field	vB_T	
E_{KL}	$vB_T\sin^2(\theta_c/2)$	*Kan and Lee* [1979]
$E_{KL}^{1/2}$	$[vB_T\sin^2(\theta_c/2)]^{1/2}$	Variant on the Kan-Lee electric field
E_{KLV}	$v^{4/3}B_T\sin^2(\theta_c/2)p^{1/6}$	*Vasyliunas et al.* [1982]
E_{WAV}	$vB_T\sin^4(\theta_c/2)$	*Wygant et al.* [1983]
E_{WAV}^2	$[vB_T\sin^4(\theta_c/2)]^2$	Variant on E_{WAV}
$E_{WAV}^{1/2}$	$[vB_T\sin^4(\theta_c/2)]^{1/2}$	Variant on E_{WAV}
E_{WV}	$v^{4/3}B_T\sin^4(\theta_c/2)p^{1/6}$	*Vasyliunas et al.* [1982]
E_{SR}	$vB_T\sin^4(\theta_c/2)p^{1/2}$	*Scurry and Russell* [1991]
E_{TL}	$n^{1/2}v^2B_T\sin^6(\theta_c/2)$	*Temerin and Li* [2006]
$d\Phi_{MP}/dt$	$v^{4/3}B_T^{2/3}\sin^{8/3}(\theta_c/2)$	This paper

Table 3. Correlations Between 20 Coupling Functions and 10 Indices[a]

Rank, f	Λ_c	Dst	AE	AU	Goes
1. $d\Phi_{MP}/dt$	−.845	−.796	.830	.765	−.760
2. E_{WAV}	−.830	−.816	.787	.734	−.751
3. E_{WV}	−.821	−.855	.798	.735	−.696
4. ε_3	−.822	−.812	.777	.718	−.737
5. E_{KL}	−.794	−.797	.759	.732	−.721
6. E_{KLV}	−.776	−.835	.772	.735	−.671
7. $E_{wav}^{0.5}$	−.818	−.714	.774	.741	−.731
8. vBs	.803	.810	−.754	−.684	.744
9. $E_{KL}^{1/2}$	−.776	−.714	.732	.720	−.697
10. E_{SR}	−.788	−.860	.756	.706	−.586
11. E_{TL}	−.775	−.859	.740	.675	−.581
12. Bs	.757	.732	−.695	−.654	.733
13. ε	−.745	−.770	.670	.632	−.567
14. ε_2	−.707	−.735	.620	.587	−.541
15. E_{WAV}^2	−.698	−.654	.628	.547	−.460
16. B_z	.644	.476	−.610	−.556	.573
17. vB_T	−.406	−.633	.385	.414	−.452
18. p	−.277	−.551	.312	.357	−.202
19. v	−.324	−.395	.374	.279	−.321
20. n	−.041	.102	.001	.093	.033

[a]The coupling functions are ranked from best ($d\Phi_{MP}/dt$) to worst (n) by the total for Λ_c, Dst, and Kp) predicted, as given in the right-hand column.

TID maximum vs. parameters

- 40 stormdates 2001-2017
- GNSS station GLSV (50.4 N, 30.5 E)

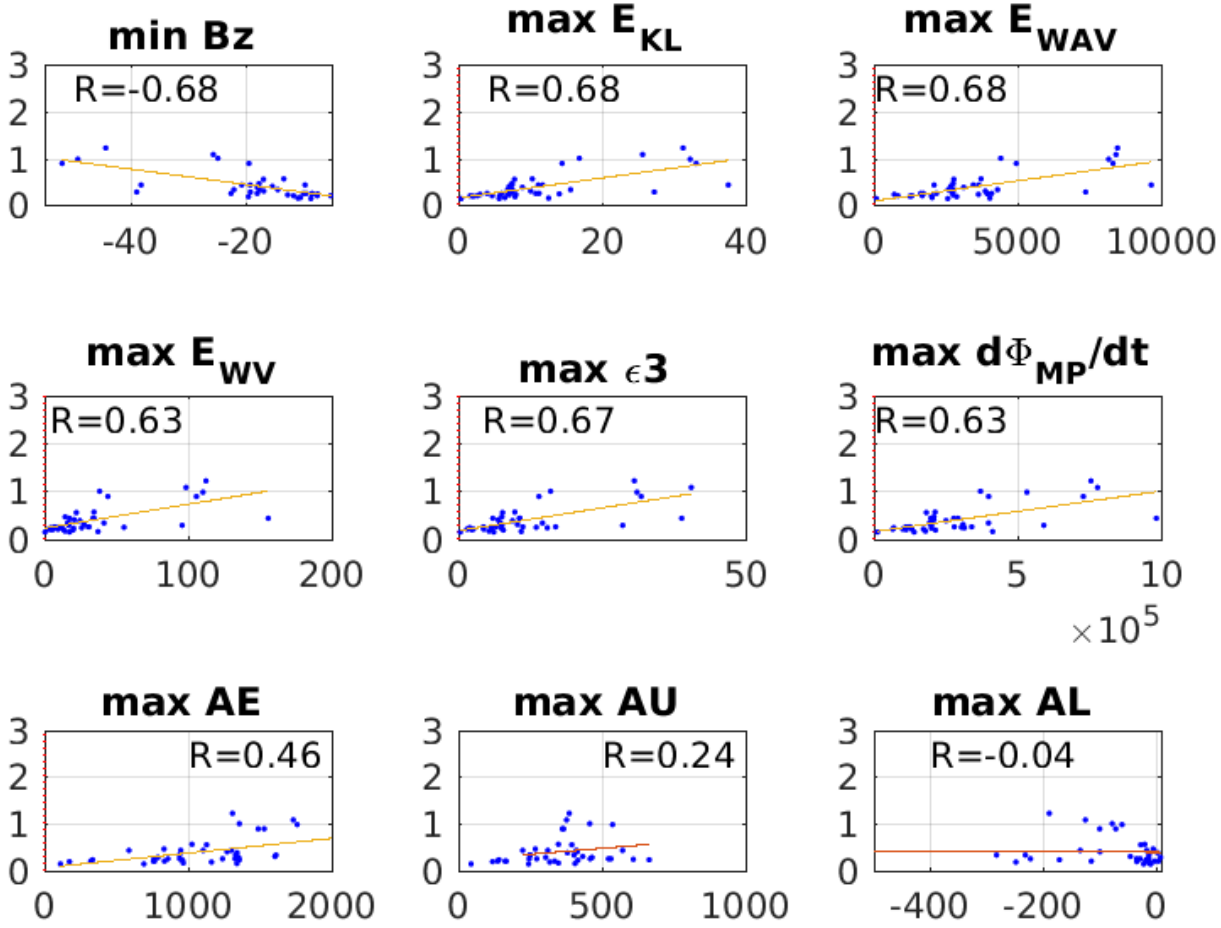

TID vs. Parameters, latitudinal dependance

- 40 stormdates (2001-2017)
- 16 stations around 8-39°E
- Not all stations have data at each storm (black=100% availability)

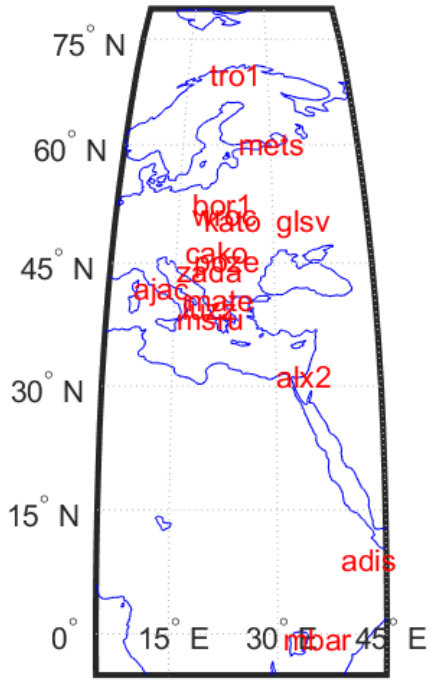

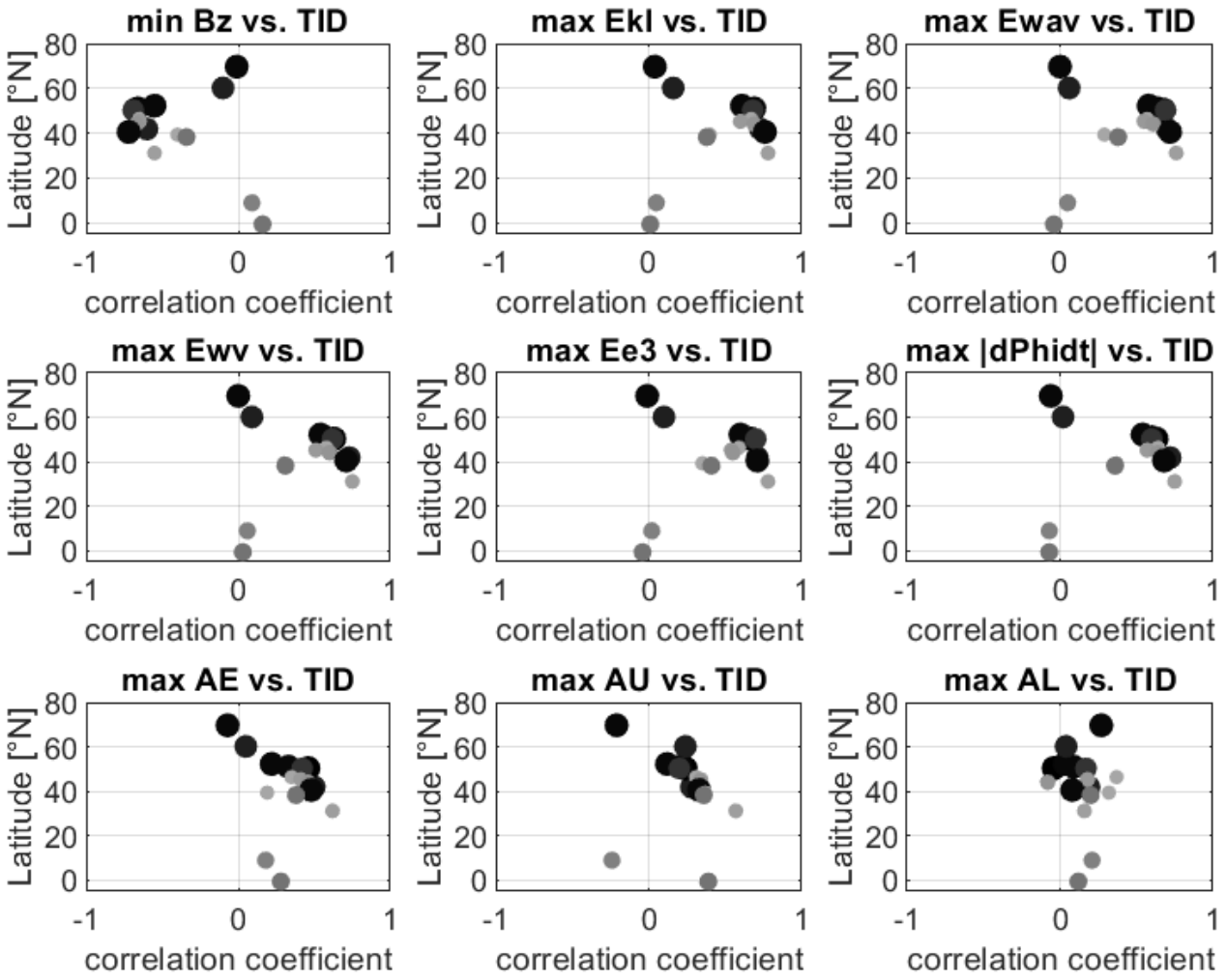

TID prediction capabilities

- Multilayer Perceptron (MLP)
  - A set of interconnected simple computing units, called neurons, interconnected by plastic links (synaptic weights) modified by a iterative training algorithm.

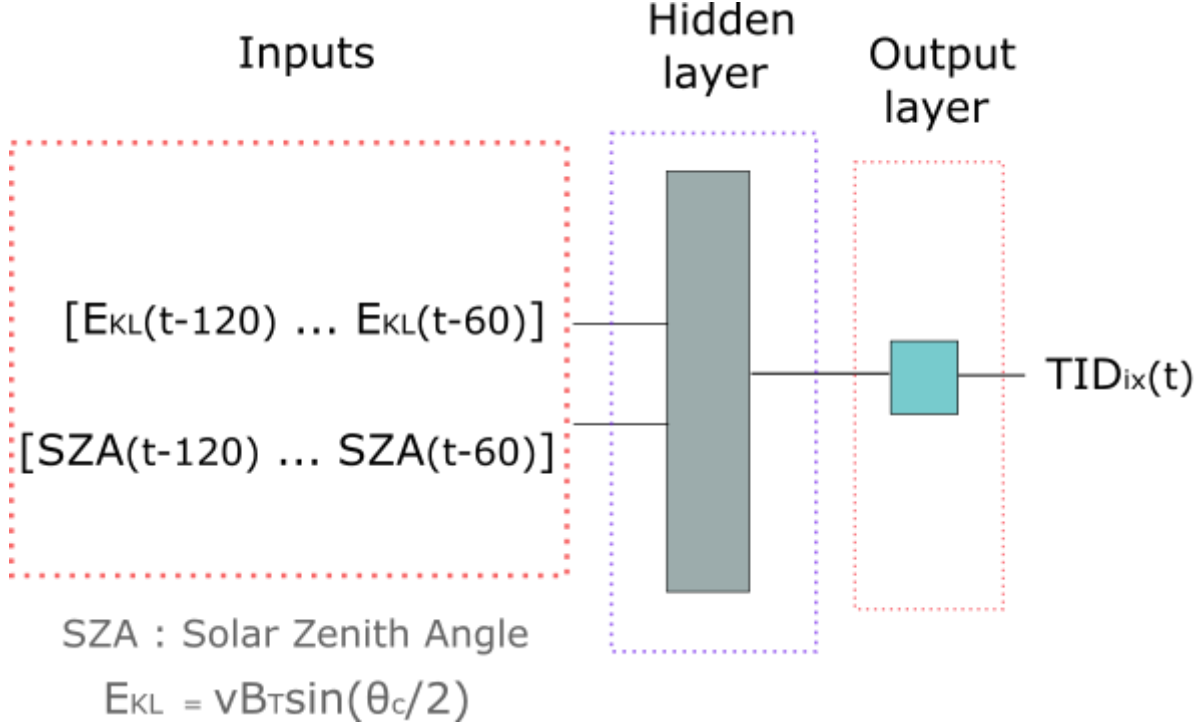

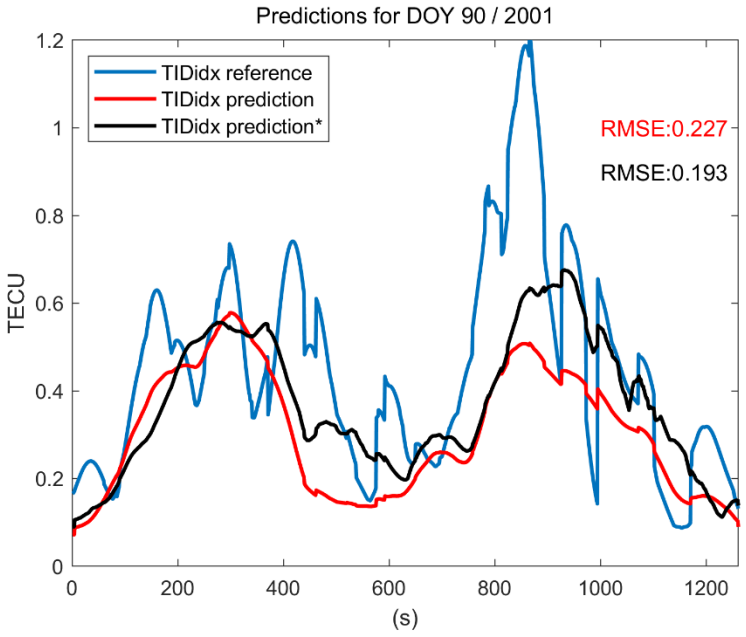

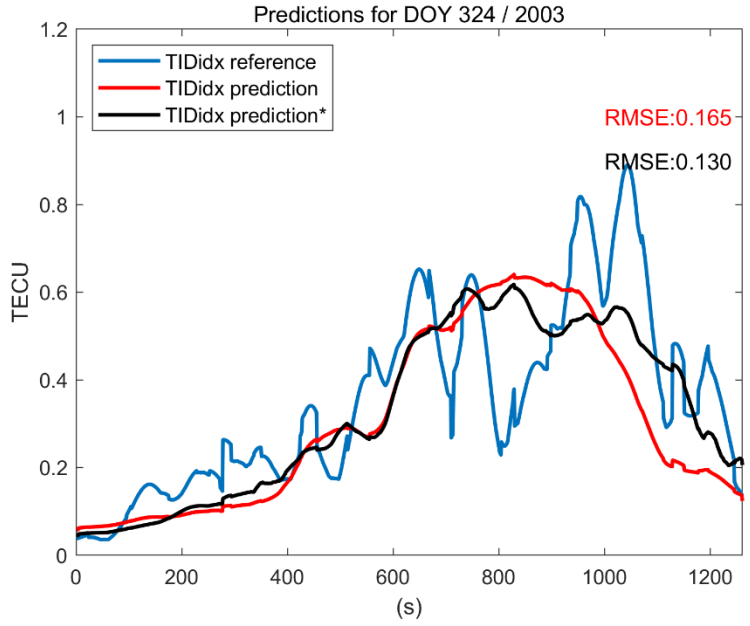

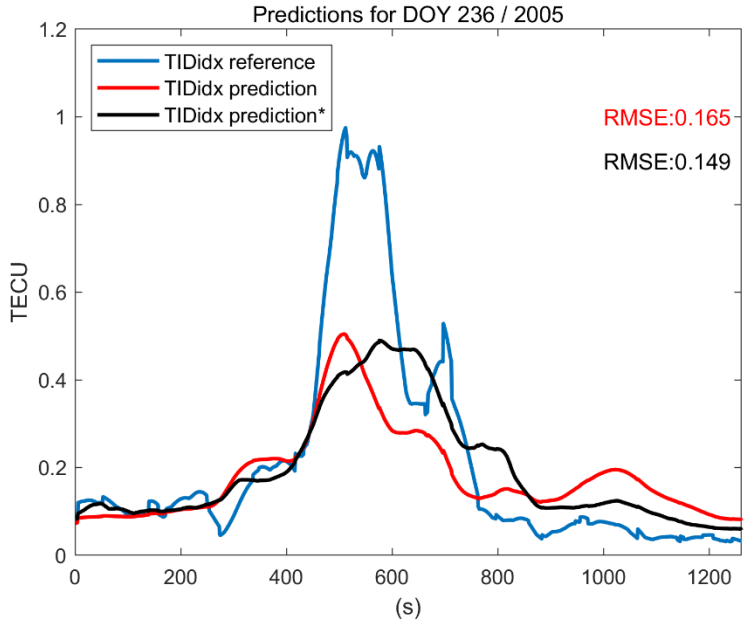

Summary and Conclusions

- LSTID activity in mid-latitudes is correlated with solar wind coupling functions with correlation values between 0.6 and 0.7
- High latitudes and low latitudes are impacted by other electrodynamic processes, overlaying the LSTID activity
- There is no big difference in the correlation of the LSTID activity with the common solar-wind-magnetosphere coupling functions
- Predictions of the general increase of LSTID activity can be done. Individual peak magnitudes are not yet predictable